Supramolecular Structure of *J*-Aggregates of a Sulfonate Substituted Amphiphilic Carbocyanine Dye in Solution: Methanol-Induced Ribbon-to-Tubule Transformation

Hans von Berlepsch,*,† Stefan Kirstein,‡ and Christoph Böttcher†

Forschungszentrum für Elektronenmikroskopie der Freien Universität Berlin, Fabeckstrasse 36 a, D-14195 Berlin, Germany, and Institut für Physik, Humboldt Universität zu Berlin, Newtonstrasse 15, D-12489 Berlin, Germany

Received: August 2, 2004; In Final Form: September 23, 2004

Replacing the pH-sensitive carboxyl substituents of amphiphilic 5,5′,6,6′-tetrachlorobenzimidacarbocyanine dyes by sulfonyl substituents promotes the formation of novel types of *J*-aggregates in aqueous solution. However, due to the dramatically reduced solubility of the examined 3,3′-bis(2-sulfoethyl)-5,5′,6,6′-tetrachloro-1,1′-dioctylbenzimidacarbocyanine (abbreviated as C8S2), aggregation in water can only be triggered by predissolution of the dye in organic solvents (e.g., methanol), the addition of surfactant (SDS), or thermal treatment. Depending on the particular preparation method used, different aggregation behavior was observed by spectroscopic and microscopic studies. Effects of methanol were studied in detail. Below a methanol concentration of ∼3.5%, the absorption spectrum shows a 2-fold split *J*-band (type **II** spectrum) characteristic for tubular structures. Above ∼3.5%, the spectrum is characterized by a pronounced *H*- and a related narrow *J*-band (type **I** spectrum) as observed for molecular aggregates with two dye molecules per unit cell (Davydov splitting). Cryo-transmission electron microscopy (cryo-TEM) revealed tubules or stacks of bilayered ribbons as the prototypical morphologies at low and high methanol concentration, respectively. By changing the methanol content of the solutions, a transition between either structures could be induced. The extremely slow kinetics allows the observation of hybrid-aggregates combining the different structural motifs within one individual entity.

I. Introduction

The design of nanostructures by self-assembly of molecules or larger supramolecular building blocks in solution has been the subject of intense studies in recent years.[1,2] A special class of self-assembled structures are the so-called *J*-aggregates formed by cyanine dyes in aqueous solutions.[3] Cyanine dyes are featured by a strongly delocalized π-electron system along the polymethine backbone that results in a high polarizability of the ground state and large oscillator strength for the transition dipole moment. On one hand, the ground state polarizability leads to strong attractive dispersion forces that favor aggregation of cyanine dye molecules.[4] On the other hand, the extended transition moments lead also to strong intermolecular coupling of the excited states.[5] As a result, an excitonic band occurs, which determines the optical properties, such as absorption and fluorescence spectroscopy.[6] The most prominent and characteristic feature of *J*-aggregates is a new excitonic transition that is red-shifted with respect to the monomers, as it was first observed by Jelley[7] and Scheibe.[8] The relation between the molecular arrangement of the dyes within the aggregate and the optical properties is given by the theory of molecular excitons (Frenkel excitons).[9] It is well-known that the single red shifted excitonic transition (the so-called *J*-band) is the result of a special geometrical arrangement of the molecules within the aggregate.[5] Depending on the molecular arrangement, different excitonic spectra can be observed and calculated, such as a symmetric splitting into two bands (Davydov splitting) for a herringbone-like arrangement[10,11] or splitting of the *J*-band into several bands for cylindrical aggregates.[12]

Recently, a new class of 5,5′,6,6′-tetrachlorobenzimidacarbocyanine dyes having different 1,1′- and 3,3′-substituents were synthesized[13−15] and spectroscopically characterized[16−18] by Dähne and co-workers. The peculiar properties of the polymethine backbone were combined with structural elements typical for amphiphilic molecules by introducing different hydrophilic and hydrophobic side groups to the chromophore. Solvophobic interactions gain significant influence here, resulting in the formation of a variety of complex molecular and supramolecular structures, which all show the typical spectroscopic features of *J*-aggregation and have therefore been termed amphi-PIPEs (amphiphiles with pigment interaction performing energy-migration).[17]

In a series of previous publications, mainly the morphology and spectroscopy of 3,3′-bis(acido-alkyl) substituted amphi-PIPEs was investigated.[19−26] Cryo-TEM was found to be an ideal technique for studying the morphologies of *J*-aggregates.

Whereas the monomer absorption spectra are almost identical for all differently substituted 5,5′,6,6′-tetrachlorobenzimidacarbocyanines,[15] the spectral behavior of the respective *J*-aggregates is strongly affected by the nature of the substituents.[14,26] Drastic spectroscopic effects were reported when the carboxy-alkyl substituents were replaced by sulfo-alkyl substituents.[13,16,26] In preliminary investigations on different derivatives,[15] Davydov splitting of the aggregate spectra as a function of dye concentration as well as time dependent effects was observed. To understand these findings, more elaborated experimental data were necessary. Thus, we carried out sys-

* To whom correspondence should be addressed. E-mail: berlepsc@chemie.fu-berlin.de.

† Forschungszentrum für Elektronenmikroskopie der Freien Universität Berlin.

‡ Humboldt Universität zu Berlin.

10.1021/jp046546f CCC: $27.50
Published on Web 11/09/2004

tematic spectroscopic and morphological investigations on respective derivatives. Here, the results obtained for the 3,3′-bis(2-sulfoethyl)-5,5′,6,6′-tetrachloro-1,1′-dioctylbenzimidacarbocyanine (C8S2):

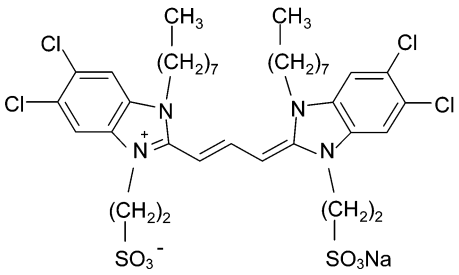

will be reported.

The strongly reduced solubility of C8S2 in water as compared to the carboxy-alkyl derivatives poses problems in the preparing of samples. Therefore, dissolution of the dye in an organic solvent prior to dilution in water was necessary to trigger aggregation. Moreover, it turned out that the particular preparation method affected the shape of spectra and the morphology of the *J*-aggregates. The investigations included studies as a function of dye concentration and methanol content in the solvent, as well as on the influence of surfactants. In all the experiments, it was necessary to take into account kinetic effects. Because of the high sensitiveness with respect to structural modifications, absorption spectra were taken as indicator at first. Later, the morphology of the aggregates was characterized by cryo-TEM and correlated with the optical spectra.

This paper is organized as follows. Section II summarizes the experimental details of material and measuring methods. Chapter III presents and discusses the experimental results. The first subsection (III.1) deals with the preparation of samples and their spectroscopic characterization, while in second subsection (III.2), the supramolecular structures as obtained by cryo-TEM are presented. Section IV presents a summary and some concluding remarks.

II. Experimental Procedures

Materials. The synthesis, purification, and analytical characterization of the C8S2 dye and other 5,5′,6,6′-tetrachlorobenzimidacarbocyanine derivatives are described in detail in ref 15. The dye C8S2 was supplied as betain salt by FEW Chemicals (Wolfen, Germany) and has been used as received. The molecular mass is 874.8 g/mol. The molar extinction coefficient in dimethylformamid (DMF) was found to be $\epsilon = 1.47 \times 10^5$ L/(mol cm). According to the manufacturer, the extinction coefficients of the sulfonated derivatives are generally lower than those of the carboxylated derivatives. Sodium dodecyl sulfate (SDS) was synthesized and purified in our laboratory to purity better than 99%. Acetonitrile (AcN) (99.8%), *cis*-1,2-dichloroethylene (97%), *N*,*N*-dimethylformamide (DMF) (99,8%), and methanol (MeOH) (99.9%, water <0.005%) were purchased from Fluka, and dimethyl sulfoxide (DMSO) (99.9%, water <0.05%) was from Acros. Double-distilled deionized water was used for preparation of the solutions.

Methods. The isotropic absorption spectra were measured with a Lambda 9 spectrophotometer and the fluorescence spectra with a luminescence spectrometer LS 50B (both from Perkin-Elmer). The linear dichroism (LD) spectra were measured by aligning the aggregates in a streaming flow of the liquid and monitoring the absorption for light polarized parallel and perpendicular to the flow direction. The measurements were performed for maximum alignment of the sample at a flow rate of about 2 cm^3/s. Details of the measuring system can be found in ref 25. The spectroscopic measurements were carried out at room temperature (21 ± 1 °C).

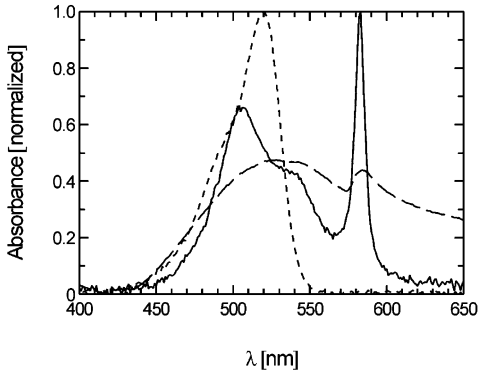

Figure 1. Absorption spectrum of C8S2 aggregates of type **I** (solid line) in a 2:1 (weight ratio) $AcN/C_2H_2Cl_2$ mixture after 3 days of aggregation. Total dye concentration: 6.4×10^{-4} M. Added is the spectrum of an aqueous dye dispersion ($[C8S2] = 2.0 \times 10^{-4}$ M, long dashes) after 3 days of stirring and the spectrum of the dye monomers (short dashes) taken in MeOH ($[C8S2] = 2.8 \times 10^{-5}$ M).

The samples for cryo-TEM were prepared at room temperature by a droplet (10 μL) of the solution being placed on a hydrophilized perforated carbon filmed grid (60s Plasma treatment at 8 W using a BALTEC MED 020 device). The excess fluid was blotted off to create an ultrathin layer (typical thickness of 100 nm) of the solution spanning the holes of the carbon film. The grids were immediately vitrified in liquid ethane at its freezing point (−184 °C) using a standard plunging device. Ultrafast cooling is necessary for an artifact-free thermal fixation (vitrification) of the aqueous solution avoiding crystallization of the solvent or rearrangement of the assemblies. The vitrified samples were transferred under liquid nitrogen into a Philips CM12 transmission electron microscope using the Gatan cryo-holder and -stage (Model 626). Microscopy was carried out at a −175 °C sample temperature using the microscopes low dose protocol at a primary magnification of 58300×. The defocus was chosen in all cases to be 0.9 μm corresponding to a first zero of the phase contrast transfer function at 1.8 nm. TEM micrographs of aggregates in $AcN/(C_2H_2Cl_2)$ mixed solvent were taken from samples deposited on carbon film at a primary magnification of 58300× and 1.2 μm defocus.

III. Results and Discussion

1. Preparation of Samples and Spectroscopic Characterization.

1.1. Two Different Types of J-Aggregates.

J-Aggregates in Polar Organic Solvent. The dye C8S2 has shown to be almost insoluble in pure water.[15] Sonification and stirring over several days yields a red-colored dispersion of the dye material (sample A in Figure 5), which showed a nearly unstructured absorption spectrum spreading over the entire wavelength range from 450 up to 650 nm (Figure 1, long dashes). Only a small shoulder at 580 nm may be an indication of partial *J*-aggregate formation. Optical microscopy revealed solid material present even after several days of stirring.

C8S2 is soluble in very polar solvents such as DMSO, DMF, or MeOH. Aggregation is not observed. As an example, the monomeric absorption spectrum of C8S2 dissolved in MeOH is shown in Figure 1 (short dashes). In less polar solvents such as chloroform or *n*-hexane, the dye is insoluble. Thus, solvents of medium polarity could be expected as promising candidates

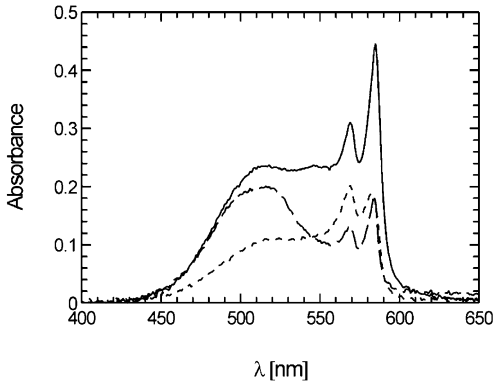

Figure 2. Absorption spectra of type **II** C8S2 aggregates 3 days after the molecularly dissolved dye has been added to water for aggregation. C8S2 was molecularly dissolved in DMSO (2.5×10^{-3} M), DMF (2.0×10^{-3} M), and MeOH (1.7×10^{-3} M; saturation concentration), respectively. Solid line: from DMSO, [C8S2] = 1.74×10^{-4} M, [DMSO] = 7 wt %; long dashes: from DMF, [C8S2] = 1.0×10^{-4} M, [DMF] = 7 wt %; short dashes: from MeOH, [C8S2] = 2.4×10^{-5} M, [MeOH] = 1.25 wt %.

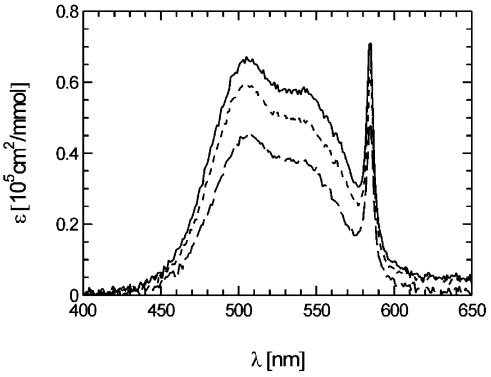

Figure 3. Absorption spectra of a 3.6×10^{-4} M C8S2 solution prepared in water from methanolic dye solution as a function of time after preparation: 1 day (solid line), 1 month (short dashes), and 3 months (long dashes). [MeOH] = 14 wt %.

for *J*-aggregation. Indeed, in dichloromethane, tetrahydrofuran, or a 2:1 mixture (weight ratio) of acetonitrile and *cis*-1,2-dichlorethylene ($AcN/C_2H_2Cl_2$), the absorption spectra indicated the formation of *J*-aggregates. A corresponding spectrum for the $AcN/C_2H_2Cl_2$ solution ([C8S2] = 6.4×10^{-4} M, after 3 days of stirring) is depicted in Figure 1 (solid line).

The absorption spectrum of *J*-aggregates in $AcN/C_2H_2Cl_2$, which we will designate as type **I** spectrum, is characterized by a narrow band peaked at 582 nm, a broad band centered at 505 nm, and a shoulder at around 545 nm. For comparison, the monomer spectrum (e.g., in MeOH) shows a single 0−0 transition with a maximum at 520 nm and a first vibrionic satellite band at around 490 nm. Since the bands at 505 and 582 nm always appeared in the same intensity ratio, it is concluded that they belong to one type of aggregate structure. Similar two-band absorption spectra have been reported for thiacarbocyanine aggregates[11,27−29] and explained by Davydov splitting.[9] They are observed when neighboring dye molecules are arranged with a nonzero angle between their transition dipole moments. The two absorption bands correspond to the sum (*H*-band at 505 nm) and difference (*J*-band at 582 nm) of the transition moments of the two molecules.[11,28,30] Hence, they should be polarized perpendicular with respect to each other.

The nature of the additional band at around 545 nm is not fully clear. A corresponding band found for solutions of thiacarbocyanine aggregates has been ascribed to residual momomers.[31] But, the band could also be caused by a second species. It seems possible that small amounts of undissolved material or other unidentified particles led to the 545 nm band.[32] Because of the unknown net concentration of aggregated dye, the absorbance values will be given in arbitrary units (and the total dye concentration in the figure captions).

J-Aggregation in Water Mediated by Organic Solvents. A completely different aggregate spectrum was found when monomeric dye solutions were first prepared in solvents such as DMSO, DMF, or MeOH and subsequently transferred into water for aggregation. The respective absorption spectra obtained after 3 days (without stirring) are shown in Figure 2. The initially broad and featureless absorption spectrum transforms into new *J*-aggregate spectra showing two prominent long-wavelength absorption bands with respective maxima at 569 and 584 nm. Aside from the differences in the peak intensity, the spectra are quite similar for the different organic solvents initially used. However, they significantly differ from the type **I** spectra obtained in $AcN/C_2H_2Cl_2$ solution and will be designated as type **II** spectra. Within the 450−550 nm wavelength range, aggregate and monomer absorptions superimpose. Different fractions of monomers may explain the strong variation in the absolute value of absorbance.

In the following, we will restrict the discussion on preparations obtained from methanolic stock solutions. It turned out that the type of *J*-aggregate that is forming depends on the amount of the monomeric solution transferred into the aqueous phase. The type **II** spectrum indicated by short dashes in Figure 2 was obtained for a sample with a content of 1.25% MeOH (B in Figure 5). Increasing the content to more than 14% (C) yields again type **I** spectra as shown in Figure 3. The main features of the spectrum correspond to those obtained in $AcN/C_2H_2Cl_2$ solution, besides some small differences: the intensity of the *J*-band relative to the *H*-band is smaller in the case of the MeOH containing aqueous solution, while the shoulder at around 545 nm is increased. Slight opalescence is also observed, indicating the presence of agglomerated dye material. Longtime storage in the dark at ambient temperature did not result in further spectral changes. Only a moderate decrease of the overall absorbance was visible within three months (cf. the dotted curves in Figure 3) indicating high stability of these (type **I**) aggregates.

The previously mentioned experiments have shown that the type of spectrum obtained is determined by the amount of the methanolic stock solution added into the aqueous phase. Because the effect could depend on both the dye and the MeOH concentration, we also checked the MeOH effect at fixed dye concentration. Two different samples were prepared starting from one particular batch of methanolic stock solution. In the first case, water was added directly, obtaining a final concentration of 3.6×10^{-4} M dye and 14% of MeOH, respectively (the same composition as the aforementioned sample C). In the second preparation (sample D), part of the methanol has been evaporated prior to the addition of water to yield a total MeOH concentration of only 2.8%. Both mixtures were left for aggregation under stirring at room temperature for 1 day before the absorption spectra were measured (Figure 4a). The first sample exhibited the typical type **I** spectrum (solid line), as expected for a high amount of MeOH (cf. also Figure 3). The sample with the reduced MeOH content (dashed line) also showed a type **I** spectrum but with strongly diminished total extinction, a broader *J*-band, and enhanced absorbance at around 545 nm. A pronounced turbidity indicated the presence of larger

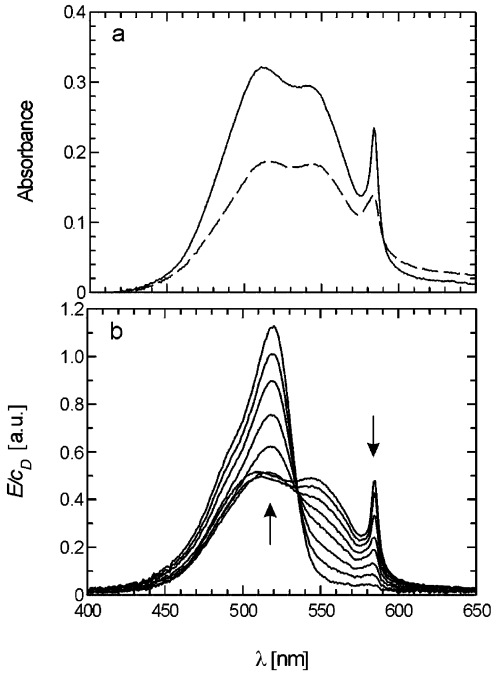

Figure 4. (a) Absorption spectrum of a 3.6×10^{-4} M C8S2 solution containing 14 wt % MeOH (solid line) prepared from methanolic dye stock solution. The dashed curve represents the absorption spectrum of a $\sim 3.9 \times 10^{-4}$ M C8S2 solution containing 2.8 wt % MeOH and prepared from the same methanolic dye stock solution by evaporating most of the solvent prior to aggregation. Both spectra were taken after 1 day of aggregation. (b) Change of absorption spectra of a 1.83×10^{-4} M C8S2 solution as a function of added MeOH. The original solution was prepared from methanolic dye solution and contained 7 wt % MeOH. The extinction, E, is normalized by the respective dye concentration, c_D. Total MeOH concentration (in wt %): 7, 15, 21, 27, 32, 36, 40, 44. Arrows indicate the effect of increasing MeOH concentration.

particles. Obviously, an essential part of the dye agglomerated and therefore was not involved in the formation of *J*-aggregates.

Because of the solubility of C8S2 in MeOH, complete disassembly into dye monomers can be expected when the MeOH concentration exceeds a certain limiting value. Figure 4b shows a set of absorption spectra of a 1.83×10^{-4} M dye solution obtained upon titration with MeOH (initial MeOH concentration 7%; sample E). Up to a MeOH concentration of 21%, mainly the hump in the absorption spectrum at 545 nm was reduced, which indicates that the fraction of the undissolved material became successively smaller. Adding still more of MeOH is accompanied by a drastic reduction of the *J*-band (584 nm), the complete disappearance of the hump (545 nm), and a strongly growing monomer band (at 520 nm). An isosbestic point can be identified at 535 nm, showing that above $\sim$21% MeOH, two species (i.e., *J*-aggregates and monomers) coexisted in an equilibrium state. At a concentration of about 40% MeOH (sample F), the aggregates were completely dissolved.

State Diagram. In the preceding sections, we have shown that the absorption spectra of C8S2 strongly depend on the conditions of sample preparation. Hence, the specification of these conditions is of fundamental importance when different samples will be compared.

There are two independent composition variables to be specified, namely, the MeOH and the dye concentration. A simple classification scheme is therefore a graphical representation in the form of a state diagram relating the observed spectral types to the corresponding MeOH (abscissa) and dye (ordinate) concentration. Since it has not been clarified if the different

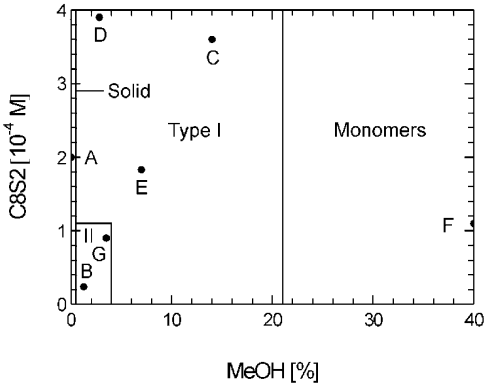

Figure 5. State diagram of C8S2 in aqueous solution as a function of MeOH and dye concentration. Four domains can be discerned, which are characterized by the presence of undissolved dye (solid), aggregates with type **II** and type **I** absorption spectra, as well as monomers.

spectra represent true equilibrium phases or not, we use the term state diagram instead of phase diagram. The respective diagram is shown in Figure 5. It should be noticed that due to the low number of samples, the state boundaries are only roughly estimated and not well-defined. Also, coexistence regions are not indicated. Nevertheless, four domains can be discerned:

(i) in the absence of methanol (e.g. in pure water), a suspension of solid dye is obtained.

(ii) At high methanol concentration (>21%), monomer solutions are formed.

(iii) At low methanol (<4%) and low dye concentrations ($<1.25 \times 10^{-4}$ M), aggregates of type **II** are observed.

(iv) For all other dye and methanol concentrations, aggregates of type **I** are found.

Samples from the type **II** domain occasionally showed also time-dependent effects in its absorption spectra. In the following section, it will be shown that these effects are caused by structural transformations between the different types of aggregates.

Type I → Type II Transformations. Because of their slow dynamics, the transitions can easily be followed by spectroscopic measurements. A quantitative analysis, however, is hampered by two difficulties. The equilibrium spectra of the different structures (type **I** and **II**) are not known a priori, and it is not clear if the pure states really exist. The second difficulty results from the interference with the insoluble material, the amount of which depends on the particular conditions of preparation.

Sample B containing 1.25% MeOH showed the characteristic split long-wavelength absorption band of the type **II** aggregates already 1 day after preparation (Figure 2). The spectrum remained stable over many days. Sample G with a slightly higher MeOH content of 3.5%, on the other hand, showed the typical type **I** spectrum after 1 day. Within several days, this more concentrated solution undergoes a transition to a type **II** spectrum, cf. Figure 6a. Because sample G shows the same characteristics after the transformation as sample B, both have been assigned to the same domain (**II**) of the state diagram (Figure 5).

According to the state diagramthe, the type **II** domain can be entered from the type **I** domain by dilution with water (keeping the MeOH to dye ratio fixed). Using (e.g., an aggregated 3.6×10^{-4} M C8S2 solution with a 14% MeOH content (same composition as sample C)), a typical type **II** spectrum is obtained 3 days after being diluted with pure water (curve indicated by short dashes in Figure 6b). Because of the long lasting kinetics of such type **I → II** transformations, it cannot be strictly suggested that the final state correponds to an equilibrium state. Presumably, the transformation process is not complete, and both types of aggregates still coexist. The

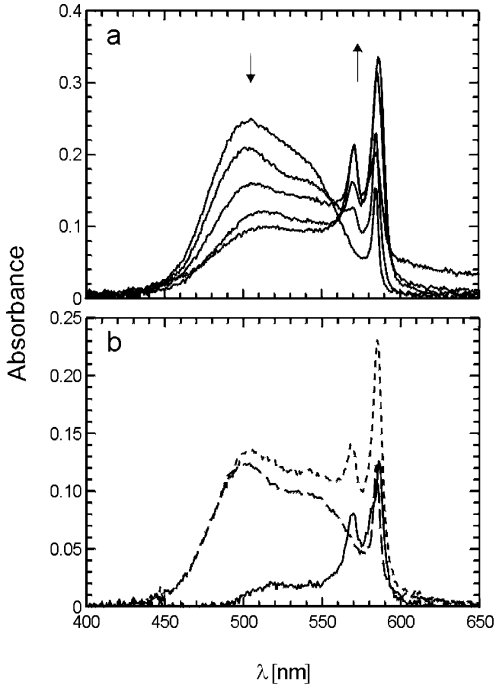

Figure 6. (a) Absorption spectra of a 9.0×10^{-5} M C8S2 solution (3.5 wt % MeOH) prepared from methanolic dye solution as a function of the passed time after preparation. The arrows indicate increasing time (in days): 1, 14, 31, 38, 51. (b) Difference spectrum (solid line) obtained by subtracting the spectrum of the original solution (type **I**, long dashes) from the measured spectrum after the type **I** → type **II** transformation (short dashes). The **I** → **II** transformation was induced by diluting an aggregated 3.6×10^{-4} M C8S2 stock solution (14 wt % MeOH) with water. Long dashes: original solution, spectrum weighted; short dashes: 3 days after dilution with water, [C8S2] = 9.0×10^{-5} M, [MeOH] = 3.5 wt %; solid line: difference spectrum.

spectrum is therefore considered to be a superposition of both spectra, whereby the pure type **II** spectrum is at first unknown, however. Subtracting the type **I** spectrum (i.e., the spectrum measured before the transformation (Figure 6b, long dashes)) from that after transformation (short dashes) should give an idea of the undisturbed type **II** spectrum. The resulting spectrum (solid line) is characterized by a split *J*-band and a plateau in the wavelength region between 520 and 550 nm. The shape of the spectrum is very similar to those reported for tubular *J*-aggregates of other 5,5′,6,6′-tetrachlorobenzimidacarbocyanine derivatives.[23,25,33] The coincidence can be considered as an indication of similar aggregate structures. The proof, however, will be provided by the cryo-TEM studies (Section III.2).

1.2. Effect of Surfactant.

The type **I** absorption spectra of solutions prepared from MeOH are typically characterized by a strong shoulder at around 545 nm. Figure 4a made clear that the shoulder becomes more pronounced when the effective solubility of the dye in the water/MeOH mixture was reduced by lowering the relative content of MeOH. On the other hand, the shoulder could be markedly reduced by preparing in $AcN/C_2H_2Cl_2$. While these findings cannot provide a conclusive explanation, they point to a solubility effect. Increasing solubility should reduce the respective band. In looking for alternative strategies to mediate the transfer of dye into the aqueous solution, we examined the effect of ionic surfactants. Note that surfactants are commonly used for controlling the solubility or dissolution rate of organic compounds in aqueous media.[34]

Figure 7 shows the spectrum of an aggregated 2.9×10^{-4} M C8S2 solution (7.5% MeOH) prior (solid line) and after titration

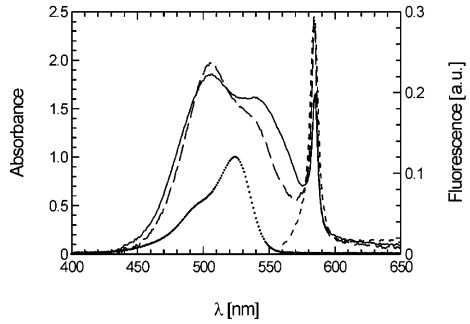

Figure 7. Change of absorbance (left ordinate) of an aggregated 2.9×10^{-4} M C8S2 solution containing 7.5 wt % MeOH (solid line) after addition of SDS (molar SDS/C8S2 mixing ratio: 20:1, long dashes). Above the cmc of SDS only monomers are detected ([C8S2] = 2.08×10^{-4} M, [SDS] = 1.6×10^{-2} M; dotted spectrum, maximum extinction normalized to $E = 1$). The fluorescence spectrum (right ordinate) of *J*-aggregates in the presence of SDS (sample with molar SDS/C8S2 mixing ratio of: 14:1) is indicated by short dashes.

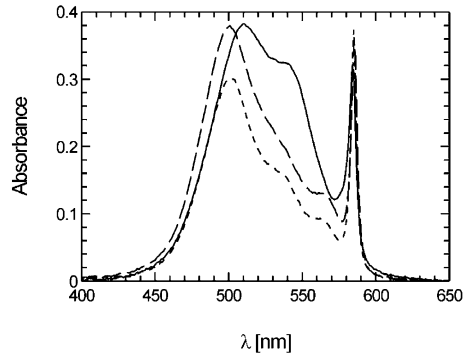

Figure 8. Shown as solid line is the absorbance of a 3.0×10^{-4} M C8S2 solution (12 wt % MeOH) prepared from methanolic dye solution in the presence of 1.3×10^{-3} M SDS. Long dashes: absorbance at room temperature after tempering the sample for 3 min at 60 °C; short dashes: after storing for further 2 days at ambient temperature.

with the anionic surfactant SDS (long dashes). The addition of SDS causes an increase of the *J*-band (584 nm) and the *H*-band (505 nm) relative to the shoulder at ∼545 nm. A fraction of material, which is thought to create this shoulder, is apparently dissolved upon SDS titration. The spectrum in the presence of SDS coincides nicely with a fresh dye solution prepared in $AcN/C_2H_2Cl_2$ (cf. Figure 1). The spectrum becomes independent of the surfactant concentration if the molar SDS/dye ratio exceeds 20:1. If the SDS concentration is further increased to reach the critical micelle concentration (8.3 mM or a ratio of 45:1, respectively), the aggregate absorption band is replaced by that of monomers (dotted curve), indicating molecular solubilization of the dye in micelles.

The fluorescence spectrum (short dashes) obtained in the presence of SDS (SDS/dye ratio of 14:1) was added to Figure 7. The spectrum does not differ from that in the absence of surfactant (not shown). The strong fluorescence is in resonance with the longest-wavelength absorption band (*J*-band at 584 nm) and of similar line width. These features are indeed well-known characteristics of *J*-aggregates.[7,8]

The remaining 545 nm shoulder in the absorbance of SDS containing samples can be further reduced by thermal treatment. The typical type **I** spectrum of a sample prepared in 1.3 mM aqueous SDS solution (SDS/dye ratio of 5:1) is shown as solid line in Figure 8. Tempering the sample for a short time (3 min at 60 °C) and cooling to room temperature gave the spectrum

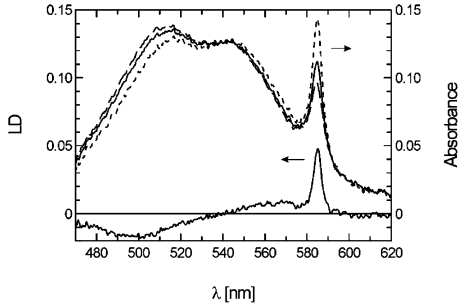

Figure 9. Absorption spectra (right ordinate) of a 3.9×10^{-4} M C8S2 sample (15 wt % MeOH) prepared from methanolic dye solution for light polarized parallel (short dashes) and perpendicular (long dashes) to the flow direction. The solid line represents the absorbance of the isotropic sample (flow switched off). The calculated linear dichroism spectrum is added (left ordinate, solid line).

indicated by long dashes. The treatment induced a slight blue-shift of the *H*-band (now at 500 nm), while the *J*-band (584 nm) remained nearly unaffected. The marked effect was a drastic reduction of the 545 nm hump accompanied by precipitation of a small amount of solid material. The coincidence of spectral changes and precipitation might support our speculation that the 545 nm hump indeed originates from incompletely dissolved dye material. Another effect of thermal treatment is the appearance of a shoulder at around 565 nm, which indicates a small contribution from coexisting type **II** aggregates. Storage at ambient temperature for two more days left the spectrum nearly unchanged (short dashes).

1.3. Linear Dichroism of Type I Aggregates.

Polarized absorption spectra can give additional information about the molecular packing in aggregates.

The measurements were restricted to *J*-aggregates showing type **I** absorption spectra only. For the polarized absorption measurements, the sample was oriented in a streaming viscous flow.[25] According to the cryo-TEM data, which will show (cf. the following section) that the aggregates are linear objects characterized by a large aspect ratio, a preferential alignment of the aggregates with their long axis parallel to the flow direction was expected. In Figure 9, the steady-state absorption spectra (right ordinate) of an aqueous C8S2 solution containing 15% MeOH are plotted for light polarized parallel (short dashes) and perpendicular (long dashes) to the flow direction. For comparison, the absorption spectrum of the isotropic sample (solid line) (i.e., with the flow switched off) is added. The linear dichroism (LD) spectrum, $LD = OD_{\parallel} - OD_{\perp}$, where $OD_{\parallel}$ and $OD_{\perp}$ represent the optical density of the sample measured with light polarized parallel and perpendicular with respect to the flow direction, was calculated and is included in the figure (left ordinate). The positive band in the LD spectrum at the position of the *J*-band (584 nm) indicates that it is polarized parallel to the long axis of aggregates, while the LD spectrum becomes negative near the short-wavelength absorption band (*H*-band) indicating a perpendicularly polarized transition. It should be noted that the absorption for perpendicularly polarized light is still substantial over the entire spectral range. The parallel-polarized transition is only reduced by approximately 40% in the perpendicular-polarized spectrum. This can be due to incomplete orientation of the aggregates or due to transitions oriented in a direction, which is neither parallel nor perpendicular to the long axis of aggregates.

The observed polarization behavior is expected for an aggregate with two molecules per unit cell. The *H*- and *J*-bands can be considered as the two perpendicularly polarized Davydov components of the split transition. The respective absorption and LD band positions do not match perfectly, however. Possibly, the species that absorb at 545 nm (shoulder) are also responsible for that effect.

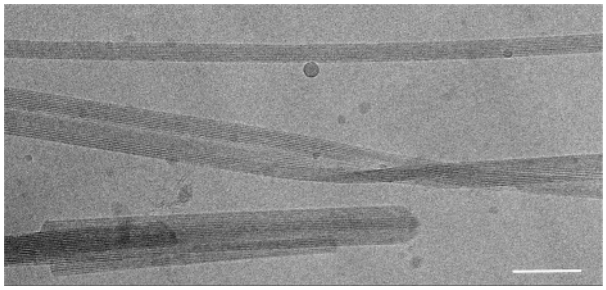

Figure 10. Cryo-TEM micrograph of a 4.3×10^{-4} M C8S2 sample (16 wt % MeOH) prepared from methanolic dye solution that shows a type **I** absorption spectrum. The sample was vitrificated 1 month after preparation. The few dark spots are surface contamination particles. Bar = 100 nm.

2. Morphology of *J*-Aggregates.

2.1. Type I Aggregates—Stacked Bilayered Ribbons.

Figure 10 shows a representative cryo-TEM image taken from a solution, which was similar in composition to sample C and characterized by the typical type **I** absorption spectrum. The micrograph reveals striped rodlike assemblies with mean total lengths in the micrometer range and typical widths ranging from 30 up to about 100 nm. The aggregates appear to be rather stiff, and twisting is rarely observed. The twisted aggregates displayed in the center of Figure 10 as well as in Figure 11 are such examples.

The most conspicuous structural characteristic of these rodlike aggregates is the pattern of stripes. A bundle of threadlike cylindrical strands as prospective structure model can be excluded because the dye molecules due to the attached octyl side chains can only aggregate into bilayer structures.[19] The thinnest cylindrical strand would be a tubule of ~8 nm cross-sectional diameter that has never been detected. The alternative structure model, which is also in accordance with the observed stripe pattern, would thus be a stack of bilayered ribbons. Similar assemblies were already observed for the C8O4 *J*-aggregates. Different approaches have been given earlier to explain the origin of the observed pattern.[19,22] Stripes can originate from the stacking of individual ribbons. They would be visible if the stacks were oriented parallel with respect to the direction of the transversing electron beam. In all other orientations, the stacking would be invisible. The aggregate displayed in Figure 11 shows these features. Stripes are only visible at the ends of the cut-out section but disappear in between. About 10 individual ribbons build up the particular multilayered assembly. The interlamellar spacing should correspond to the individual thickness of the ribbons. The obtained value of 3.2 ± 0.2 nm is in the order of magnitude expected for an arrangement of dye molecules in bilayers in which the chromophores are stacked in plane-to-plane orientation and the octyl chains are intercalated between the layers to prevent contact with the surrounding aqueous medium. All amphi-PIPEs should self-aggregate into bilayer structures.[19]

However, the mayor fraction of the assemblies shows stripe patterns of demonstrable different origin, see, for example, Figure 10. The periodicity of the stripes here is not homogeneous but varies within a broad range from ~3.5 nm down to about 2 nm. Such patterns with subbilayer spacings may result from the constituent monolayers and/or the superposition of misaligned mono- and bilayers (Moiré pattern) forming the stacks.[19,22]

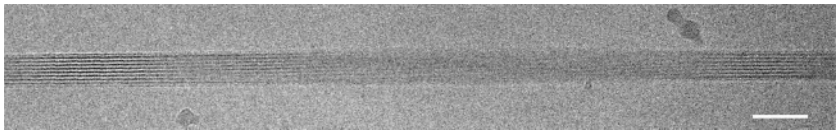

Figure 11. Cryo-TEM micrograph of a stacked assembly of bilayers that is continuously twisted. The sample was aggregated in SDS containing water from methanolic dye solution and vitrificated 4 months after preparation. [C8S2] = 2.5×10^{-4} M; [MeOH] = 11.5 wt %; molar SDS/C8S2 mixing ratio: 17:1. Bar = 50 nm.

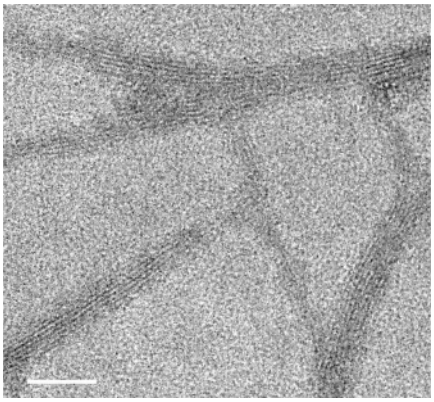

Figure 12. TEM micrograph of *J*-aggregates prepared in $AcN/C_2H_2Cl_2$ mixture showing a type **I** absorption spectrum. Bar = 50 nm.

While the addition of SDS affected the absorbance, in particular in the wavelength region around 545 nm (cf. Figure 7), a noticeable effect on the morphology of the assemblies was not observed. This surprising finding could be due to a size exclusion effect. It has frequently been reported that particles larger than approximately 300 nm in diameter are excluded from the cryo-preparation by the blotting process and are therefore not detectable in the microscope.[35] When this particular fraction of material is responsible for the absorption at 545 nm, then in fact a morphological effect of SDS should not be observed.

The second important finding is that SDS does not influence the stacking structure of the aggregates. The twisted aggregate shown in Figure 11, for example, obtained from an SDS containing solution, resembles exactly those preparations without SDS. Interestingly, it has been found in case of the C8O4 derivative earlier[22] that the addition of SDS can strongly influence the supramolecular organization of the aggregates. Here, the surfactant induced a full separation of the formerly stacked assemblies into isolated ribbons. The different behavior in the case of C8S2 points to a stronger face-to-face attraction between the ribbons. This is in particular interesting because stabilization of the assemblies by hydrogen-bonding networks can be excluded for the sulfonated derivative C8S2. Hydrogen bonding was considered to promote stacking in the case of the carboxy-butyl derivative C8O4.[19] Thus, we believe that the attractive dispersion forces between the extended π-electron systems of neighboring bilayers faces drive their stacking. In the general context of self-assembly of amphiphilic solutions, the stacking of ribbons can be attributed to the requirement of the system to optimize its interfacial energy. The cost in the surface energy of the ribbons with respect to the aqueous environment is obviously balanced by the energy gain due to the face-to-face attraction on stacking.

Unfortunately, the direct observation of the native aggregates in $AcN/(C_2H_2Cl_2)$ by cryo-TEM is experimentally hampered since vitrification of the particular solvent cannot be achieved.[35] However, preparations of air-dried samples (Figure 12) showed a stripe motif with typical 3.2 ± 0.2 nm spacing. This is in very good agreement with the respective structures revealed by cryo-TEM (Figures 10 and 11).

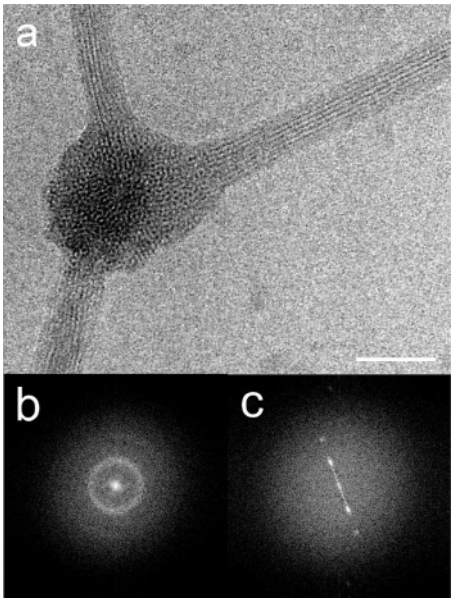

Figure 13. (a) Cryo-TEM micrograph of cross-linked aggregates. The junction connects three striped aggregates and shows a granular structure. The Fourier transforms taken from (b) the granular clot and (c) the stripe pattern gives in either case a typical repetition period of 3.2 nm. Same sample as in Figure 11. Bar = 50 nm.

2.2. Bilayer Fragments Forming Clot-Like Assemblies.

An interesting novel structural motif is clot-like features (Figure 13a), which are often observed at the ends of striped aggregates and sporadically serve as cross-linking motifs between aggregates. The clots have been found in solutions with type **I** absorption spectrum in the absence or in the presence of SDS, indicating that they are not influenced by the surfactant. We were neither able to tune their number and size nor to identify them spectroscopically. Closer inspection reveals a granular fine structure. Fourier transforms taken from such granular patterns as well as from neighboring aggregates (Figures 13b,c) give identical spacings of 3.2 ± 0.2 nm, which correspond to the typical thickness of a molecular bilayer. We speculate that the clots are isotropically ordered assemblies of bilayer fragments. Because of the frequently observed fusion with other stacked multilayered assemblies, one might consider the clots as being precursors in the assembling or even disassembling process.

2.3. Type II Aggregates—Tubules.

We will now discuss the morphologies of the samples, which showed a type **I** → type **II** spectral transformation. The detected changes in the absorbance (cf. Figure 6a) are accompanied by the appearance of new morphologies. Representative cryo-TEM images are presented in Figures 14−16. The sample (same composition as G) was prepared from methanolic dye solution and stored for one month. Figure 14 shows tubular aggregates. The majority is single-walled with a wall thickness of 3.4 ± 0.2 nm and typical lengths of about 1 μm. Cross-sectional

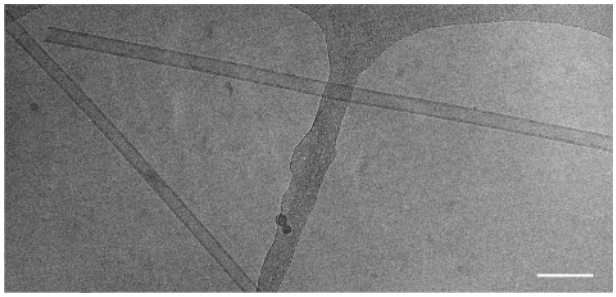

Figure 14. Cryo-TEM micrograph of a 9.0×10^{-5} M C8S2 solution (3.5 wt % MeOH) showing a type **II** absorption spectrum. The sample was prepared from methanolic dye solution and has been vitrificated 1 month after preparation. Bar = 100 nm.

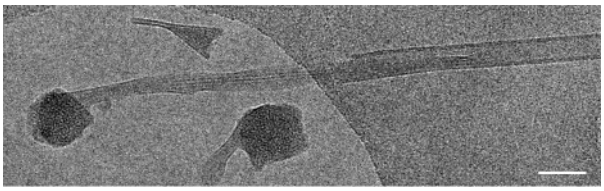

Figure 15. Cryo-TEM micrograph of a hybrid-aggregate combining three different structural motifs in one individual entity. Same sample as in Figures 14. Bar = 50 nm.

diameters ranging between 27.0 and 28.5 ± 0.5 nm were estimated, indicating a slight polydispersity. Figure 15 presents a hybrid-aggregate, which combines three different structural motifs in one individual entity. The structural compartments, which tend to gradually fuse into each other, descriptively consist of a granular clot, a stack of bilayers, and a single-walled tubule (from left to right). Similar hybrid-aggregates coexist with entities showing one of the motifs in a completely uniform manner.

The concurrent emergence of the tubular structural motif and the splitting of the *J*-band is an explicit indication that the spectral changes are caused by a morphological transition of the stacked ribbonlike type **I** aggregates into tubular type **II** aggregates. The split *J*-band appeared earlier as a characteristic feature of tubular aggregates of the C8O3 derivative[19,25] and a different sulfonate substituted 5,5′,6,6′-tetrachloro-1,1′-dioctylbenzimidacarbocyanine derivative.[33] Because of the coexistence of species with different morphologies, however, the spectrum is more complicated in the present case. The additional component in the absorption spectrum at around 500 nm (cf. the discussion of Figure 6b) is due to the *H*-band of the coexisting type **I** aggregates. Their *J*-band (584 nm) is invisible because it is buried within the strong *J*-bands of the tubules.

An interesting aspect of the MeOH-induced transformation between the two types of aggregates is its slow kinetics. *J*-aggregates are supramolecular entities, whose constituents are linked through reversible connections, which may undergo assembly and disassembly in response to external factors. The extremely slow kinetics originates from the multiplicity of molecular interactions in the aggregates and allows the observation of intermediate states of aggregation, or more generally, to learn about the mechanism of structure formation. Figure 16, for instance, shows a tubule enclosing a helically wound bilayered ribbon. Such types of hybrid-aggregates have frequently been observed. One might speculate that they are intermediate states during the conversion of the planar multistacks into single-walled tubules. Since isolated ribbons that wind up into tubules or something else were never observed, we conclude that the structures rearrange via complete intermediate disassembly of the stacked ribbons.

The addition of alcohols strongly affects *J*-aggregation of all amphi-PIPEs studied so far. Hereby, methanol plays an outstanding role, and this is also the case in the context of C8S2 aggregation. The effect of alcohols is related to their surface activity, which enforces the alcohol molecules to adsorb preferably at the interface of aggregates and the surrounding solvent. As observed earlier for C8O3 *J*-aggregates,[23,24] the incorporation of alcohols can affect the packing of chromophors on the molecular as well as the supramolecular level. However, in contrast to the C8O3 *J*-aggregates, whose tubular topography prevails up to a total of at least 20% MeOH,[23] C8S2 tubules lose their stability at a methanol content of as low as ∼4% (cf. the state diagram). Obviously, a critical MeOH concentration exists up to which the incorporation of alcohol molecules into the curved structure is tolerated without a structural transformation. A numerical value for the critical molecular mixing ratio cannot be given because of the unknown amount of incorporated MeOH, but it is likely that the comparatively higher stability of C8O3 tubules against MeOH is due to stabilizing effects of intermolecular hydrogen bonds formed by carboxyl side groups, which do not exist in sulfonated derivatives.

IV. Summary and Conclusions

Exchanging the carboxyl substituents of amphiphilic tetrachlorobenzimidacarbocyanines by sulfonyl substituents has a strong effect on the dyes solubility in water. Whereas pH tuning (addition of NaOH) of the carboxyl groups is necessary to accomplish solubility of the C8O3 and C8O4 amphi-PIPEs in water,[16,19] the examined derivative C8S2 has such a low solubility that dissolution in organic solvent prior to aggregation is necessary to trigger aggregation in water. MeOH turned out to be a suitable solvent, but its concentration in the final solution appeared to be a structure-determining factor. Depending on the MeOH concentration, *J*-aggregation is characterized by different absorption spectra and supramolecular morphologies.

The structure of C8S2 in aqueous solution appears highly complex because three different types of mesoscopic particles and traces of incompletely dissolved materials commonly coexist. In this respect, the present derivative differs fundamentally from the formerly investigated carboxylated amphi-PIPEs (C8O3, C8O4) that only form one type of aggregate even when alcohols are present.[23] The coexistence of different types of particles explains the complexity of the absorption spectrum of the C8S2 solutions.

Below ∼3.5%, the absorption spectrum (of type **II**) shows a 2-fold split *J*-band as it is characteristic for tubular aggregate structures. Cryo-TEM revealed three different structural motifs, namely, small granular clots, striped assemblies, and tubules.

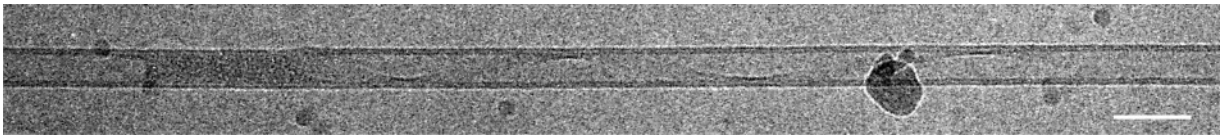

Figure 16. Cryo-TEM micrograph of a C8S2 tubule into which a helically wound bilayered ribbon is embedded. The dark spots are surface contamination particles. Same sample as in Figures 14 and 15. Bar = 50 nm.

The tubules are single-walled and slightly polydisperse in diameter, and they are responsible for the *J*-band splitting. The striped assemblies are composed of stacked bilayered ribbons. The clots turned out to be isotropically ordered assemblies of bilayer fragments. Above ~3.5% of MeOH, tubular aggregates are not found anymore, while the clots and the striped assemblies survive. The absorption spectrum is characterized by a pronounced *H*- and a related narrow *J*-band (type **I**) as it is typical for a molecular aggregate with two dye molecules per unit cell.

The investigations have shown that a critical MeOH concentration exists above which the incorporation of alcohol molecules destabilizes the tubular structure and drives a structural transition. The carboxylated derivative C8O3 does not show a comparable effect. The higher stability of the C8O3 tubules against MeOH is probably due to a stabilizing effect of intermolecular hydrogen bonds formed by carboxyl side groups. Because of the slow kinetics of the MeOH-induced structural transformations in the case of C8S2, it is possible to observe new hybrid-aggregates combining all the different structural motifs within one individual entity. The morphological transformations are generally accompanied by structural changes on the molecular scale and thus explain why time dependent absorption spectra have been found in early work.[15]

Interestingly, *J*-aggregates of C8S2 are also found in nonaqueous environment ($AcN/C_2H_2Cl_2$). Addition of the anionic surfactant SDS has no noticeable effect on the aggregate morphology.

Acknowledgment. The authors thank Prof. S. Dähne for the generous gift of some of the C8S2 dye samples used. We are further grateful to A. Pugžlys for the LD measurements. This work has been supported by the Deutsche Forschungsgemeinschaft (SFB 448 "Mesoskopisch strukturierte Verbundsysteme").

References and Notes

(1) Lehn, J.-M. *Supramolecular Chemistry, Concepts, and Perspectives*; VCH: Weinheim, 1995.

(2) Balzani, V.; Scandola, F. *Supramolecular Photochemistry*; Ellis Horwood: Chichester, 1991.

(3) *J-Aggregates*; Kobayashi, T., Ed.; World Scientific: Singapore, 1996.

(4) Bach, G.; Dähne, S. Cyanine dyes and related compounds. In *RODD's Chemistry of Carbon Compounds*, 2nd ed.; Sainsbury, M., Ed.; Elsevier: Amsterdam, 1997; Vol. IVB (2nd Suppl.), p 383.

(5) Czikkely, V.; Försterling, H. D.; Kuhn, H. *Chem. Phys. Lett*. **1970**, *6*, 11.

(6) Moll, J.; Dähne, S.; Durrant, J. R.; Wiersma, D. A. *J. Chem. Phys*. **1995**, *102*, 6362.

(7) Jelly, E. E. *Nature* **1936**, *138*, 1009.

(8) Scheibe, G. *Angew. Chem*. **1937**, *50*, 51.

(9) Davydov, A. S. *Theory of Molecular Excitons*; Plenum Press: New York, 1971.

(10) Saito, K.; Ikegami, K.; Kuroda, S.; Tabe, Y.; Sugi, M. *Jpn. J. Appl. Phys.* **1991**, *30*, 1836.

(11) Kirstein, S.; Möhwald, H. *Adv. Mater*. **1995**, *7*, 460.

(12) Bednarz, M.; Knoester, J. *J. Phys. Chem. B* **2001**, *105*, 12913.

(13) De Rossi, U.; Moll, J.; Spieles, M.; Bach, G.; Dähne, S.; Kriwanek, J.; Lisk, M. *J. Prakt. Chem*. **1995**, *337*, 203.

(14) Pawlik, A.; Kirstein, S.; De Rossi, U.; Dähne, S. *J. Phys. Chem. B* **1997**, *101*, 5646.

(15) Pawlik, A.; Ouart, A.; Kirstein, S.; Abraham, H.-W.; Dähne, S. *Eur. J. Org. Chem*. **2003**, 3065.

(16) De Rossi, U.; Dähne, S.; Meskers, S. C. J.; Dekkers, H. P. J. M. *Angew. Chem*. **1996**, *108*, 827.

(17) Spitz, C.; Knoester, J.; Ouart, A.; Dähne, S. *Chem. Phys.* **2002**, *275*, 271.

(18) Lampoura, S. S.; Spitz, C.; Dähne, S.; Knoester, J.; Duppen, K. *J. Phys. Chem. B* **2002**, *106*, 3103.

(19) von Berlepsch H.; Böttcher, C.; Ouart, A.; Burger, C.; Dähne, S.; Kirstein, S. *J. Phys. Chem. B* **2000**, *104*, 5255.

(20) von Berlepsch, H.; Böttcher, C.; Ouart, A.; Regenbrecht, M.; Akari, S.; Keiderling, U.; Schnablegger, H.; Dähne, S.; Kirstein, S. *Langmuir* **2000**, *16*, 5908.

(21) Kirstein, S.; von Berlepsch, H.; Böttcher, C.; Burger, C.; Ouart, A.; Reck, G.; Dähne, S. *Chem. Phys. Chem.* **2000**, *1*, 146.

(22) von Berlepsch, H.; Regenbrecht, M.; Dähne, S.; Kirstein, S.; Böttcher, C. *Langmuir* **2002**, *18*, 2901.

(23) von Berlepsch, H.; Kirstein, S.; Böttcher, C. *Langmuir* **2002**, *18*, 7699.

(24) von Berlepsch, H.; Kirstein, S.; Böttcher, C. *J. Phys. Chem. B* **2003**, *107*, 9646.

(25) von Berlepsch, H.; Kirstein, S.; Hania, R.; Didraga, C.; Pugžlys, A.; Böttcher, C. J. Phys. Chem. B **2003**, *107*, 14176.

(26) Ouart, A. Ph.D. Thesis, Humboldt-Universität, Berlin, 2000.

(27) Hada, H.; Honda, C.; Tanemura, H. *Photogr. Sci. Eng*. **1977**, *21*, 83.

(28) Scheblykin, I. G.; Drobizhev, M. A.; Varnavsky, O. P.; van der Auweraer, M.; Vitukhnovsky, A. G. *Chem. Phys. Lett*. **1996**, *261*, 181.

(29) Janssens, G.; Touhari, F.; Gerritsen, J. W.; van Kempen, H.; Callant, P.; Deroover, G.; Vandenbroucke, D. *Chem. Phys. Lett*. **2001**, *344*, 1.

(30) Basko, D. M.; Lobanov, A. N.; Pimenov, A. V.; Vitukhnovsky, A. G. *Chem. Phys. Lett.* **2003**, *369*, 192.

(31) Kirstein, S.; Möhwald, H. *Makromol. Chem., Macromol. Symp.* **1991**, *46*, 463.

(32) Various findings indicate an incomplete dissolution of the dye in $AcN/C_2H_2Cl_2$. The molar extinction of the *J*-band of $\epsilon_J \approx 5.6 \times 10^4$ cm^2/mmol amounts to only a few percent as compared to the corresponding values of C8O3 and C8O4 aggregates in aqueous solution. Besides, the 6.4×10^{-4} M C8S2 solution in $AcN/C_2H_2Cl_2$ shows a slight turbidity. Longer stirring (up to one week) increased the transparency and the value of extinction.

(33) Didraga, C.; Pugžlys, A.; Hania, R.; von Berlepsch, H.; Duppen, K.; Knoester, J. *J. Phys. Chem. B*, **2004**, *108*, 14976.

(34) Yalkowski, S. H. *Solubility and Solubilization in Aqueous Media*; American Chemical Society: Washington, DC, 1999.

(35) Talmon, Y. *Ber. Bunsen-Ges. Phys. Chem*. **1996**, *100*, 364.